Single domain strain relaxed $PrScO_3$ template on miscut substrates

C. M. Folkman, R. R. Das, and C. B. Eom[a)]
Department of Materials Science and Engineering, University of Wisconsin-Madison, Madison, Wisconsin 53706

Y. B. Chen and X. Q. Pan
Department of Materials Science and Engineering, University of Michigan, Ann Arbor, Michigan 48109

(Received 1 September 2006; accepted 16 October 2006; published online 27 November 2006)

The authors have *grown strain relaxed* epitaxial template of a rare-earth scandate, $PrScO_3$, on miscut (001) $SrTiO_3$ and (001) $(LaAlO_3)_{0.3}-(Sr_2AlTaO_3)_{0.7}$ substrates by pulsed laser deposition of $PrScO_3$ buffer layers followed by postannealing and overlayer growth. X-ray diffraction exhibits that the $PrScO_3$ is a *single domain* with bulk lattice parameters and the out-of-plane crystalline quality is comparable with $SrTiO_3$ single crystals. Cross-sectional transmission electron microscopy micrographs show dislocation-free overlayers containing boundaries with very small in-plane misalignment. The growth of strain relaxed rare-earth scandate templates with controlled lattice parameters offers strain and domain engineering of epitaxial multifunctional oxide thin films. © *2006 American Institute of Physics*. [DOI: 10.1063/1.2396920]

Strain engineered epitaxial oxide thin films have drawn great attention due to the enhancement of ferroelectric, ferromagnetic, and superconducting properties in strained perovskite thin films.[1–3] The most versatile method of inducing strain in the lattice structure can be achieved by heteroepitaxy of thin films on substrates with engineered lattice mismatch.

Recently, there has been an interest to grow epitaxial perovskite oxide thin films on orthorhombic rare-earth scandate ($REScO_3$) substrates to improve the performance of oxide devices.[1–3] The lattice parameters of $REScO_3$ substrates can be tuned with the selection of a lanthanide rare-earth ion, for example, $LaScO_3$ with $a_o^p=4.054$ Å and $c_o^p=4.049$ Å and $DyScO_3$ with $a_o^p=3.94$ Å and $c_o^p=3.95$ Å (p denote pseudocubic, $a_o^p=\sqrt{(a_o^2+b_o^2)}/2$ and $c_o^p=c_o/2$).[1] Previously, we have reported strained epitaxial $BaTiO_3$ on $GdScO_3$ and $DyScO_3$, which exhibits higher transition temperature (550 °C) with enhanced polarization.[2] Other $REScO_3$ single crystals, such as $LaScO_3$ are not commercially available for reasons that these scandate single crystals cannot be grown via the Czochralski method because of high melting temperatures.[3] These unavailable $REScO_3$'s allow us to study transition temperature versus strain phase diagrams for selected ferroelectrics on anisotropic substrates.[4] For example, Wang and Zhang[4] predicted that application of simultaneous tensile and compressive biaxial strain on $BaTiO_3$ and $PbTiO_3$ can result in a uniaxial polarization parallel to the surface.

An alternative to producing single crystal $REScO_3$'s is to deposit the strain relaxed scandate thin film template on a common perovskite substrate. This approach avoids the challenges of creating bulk single crystals and the high costs of raw materials, while opening the possibility for integration of strained multifunctional oxide heterostructures with controlled properties. Terai *et al.*[5] reported annealed $BaTiO_3$ thin films on $SrTiO_3$ substrates that were used as compliant buffer layers for strained $Ba_xSr_{1-x}TiO_3$, where lattice parameters can be tuned up to ~4 Å with increasing Ba concentration.

In this letter, we report the growth and properties of strain relaxed single domain $PrScO_3$ (PSO) templates on $SrTiO_3$ (STO) and $(LaAlO_3)_{0.3}-(Sr_2AlTaO_3)_{0.7}$ (LSAT) miscut substrates. The lattice parameters of PSO are $a_o=5.770$ Å, $b_o=5.602$ Å, and $c_o=8.010$ Å or $a_o^p=4.021$ Å and $c_o^p=4.005$ Å,[1] which are close to those of pervoskite ferroelectric materials. $RESc_3$'s have high thermal stability[3] and low dielectric constants.[6] Furthermore, the domain structure of the $RESc_3$ can be engineered into a single domain film employing miscut substrates. Ideal template layers for strain engineering will behave as a single crystal with regard to lattice parameters, domain structure, defect densities, surface smoothness, and crystalline quality.

PSO epitaxial thin films were deposited on miscut (001) STO substrates toward [100], where miscut angle $\alpha=0.2°$, 0.5°, 1.0°, 2.0°, and 4.0°, as shown in Fig. 2(a). The surfaces were TiO_2 terminated using a process described elsewhere.[7] The PSO template was constructed according to a three-step process schematically represented in Fig. 1. First, a 300 Å PSO buffer (PSO-B) layer was deposited *in situ* at 250 mTorr O_2 atmosphere and 900 °C by pulsed laser deposition with a KrF excimer laser. The laser energy density was 3.3 J/cm^2 and the pulse repetition rate was 5 Hz. Next, the PSO buffer was annealed *ex situ* (PSO-AB) at 1200 °C in air for 1 h to improve the crystalline quality of the as-deposited PSO buffer layer. Finally, the 1000 Å PSO overlayer template (PSO-T) was deposited on the annealed buffer using the previous deposition parameters. The PSO buffer layer

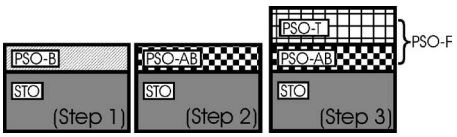

FIG. 1. Schematic of three-step fabrication process for the strain relaxed PSO template layer: (1) thin layer deposition of PSO on the STO substrate (PSO-B), (2) postannealing (PSO-AB), and (3) PSO overlayer deposition (PSO-T) on top of the postannealed thin PSO; the entire structure is named PSO-F.

[a)]Author to whom correspondence should be addressed; electronic mail: eom@engr.wisc.edu

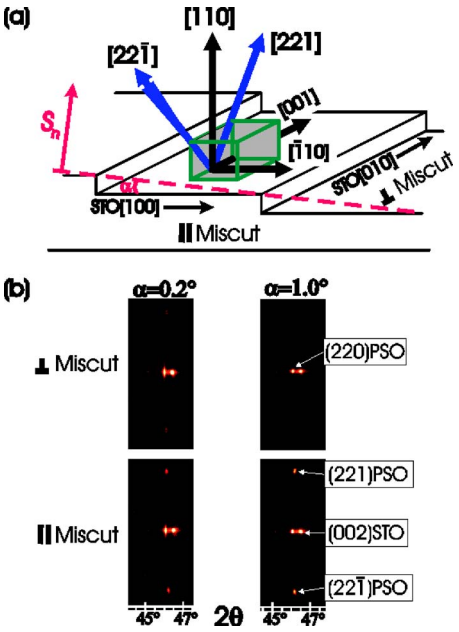

FIG. 2. (Color online) Schematic (a) of the primary PSO domain with respect to the miscut direction of the STO substrate. The miscut angle is defined as the angle between surface normal S_n and STO [100]. (b) 2D images of x-ray diffraction reflections from PSO (PSO-F) on miscut (001) STO substrates (α=0.2° amd 1.0°) both parallel (∥) and perpendicular (⊥) to the substrate miscut direction.

and template constituted the final structure (PSO-F). In addition, to demonstrate the versatility of possible substrate materials, an identical PSO template was processed on miscut (001) LSAT substrates (α=2.0°). The LSAT substrate was annealed in oxygen at 1100 °C for 1 h without chemical etching to prepare the surface for epitaxial growth.[8]

The epitaxial arrangements, three-dimensional strain states and crystalline qualities of the PSO were determined by four-circle x-ray diffraction with a two-dimensional (2D) area detector and a four-bounce monochromator and by transmission electron microscopy (TEM). The PSO films were analyzed according to *Pbnm* crystal symmetry (all indices are based on orthorhombic unit cell).[1] Figure 2(b) shows 2D images of diffraction peaks from PSO (PSO-F) on miscut (001) STO substrates (α=0.2° and 1.0°) parallel (∥) and perpendicular (⊥) to the substrate miscut direction. 2D area detector allows access to the on-axis and off-axis reflections simultaneously. The only diffraction spots detected normal to the substrates are *hh*0 of PSO, which is a typical growth direction of distorted perovskites on cubic substrates.[9]

The in-plane texture of the PSO domain was found to be strongly dependent on the substrate miscut α. Due to the orthorhombic structure of PSO, a single domain (220) PSO thin film should exhibit off-axis (221) reflections at every 180° (twofold symmetry) in the plane. 2D x-ray diffraction measurements at orthogonal in-plane directions (or parallel and perpendicular to the miscut direction) determine the in-plane domain structures of PSO. PSO on low miscut ($\alpha \leqslant 0.5°$) STO substrates (0.2° shown in the figure) displayed 221 reflections in x-ray scans parallel and perpendicular to the miscut direction (every 90°) indicating the presence of two domains rotated 90° apart. In contrast, PSO on high miscut STO substrates ($\alpha \geqslant 1.0°$) (1.0° shown in the figure) displayed the PSO 221 reflection only parallel to the miscut

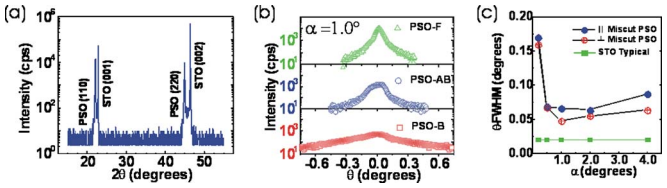

FIG. 3. (Color online) X-ray diffraction θ-2θ scan (a) for the PSO-F on the miscut (001) STO substrate (α=1.0°), (b) rocking curves of the PSO (220) reflection after each period in the three-step process, and (c) FWHM of the PSO-F (220) rocking curve versus STO miscut angles (α) of STO substrates.

direction. This indicates that *single domain* nucleation with in-plane $[001]_{PSO}$ perpendicular to the miscut direction is energetically favorable by increased substrate miscut, as illustrated in Fig. 2(a). Selected area electron diffraction (SAED) and TEM diffraction contrast imaging also confirm the x-ray diffraction (XRD) results. The same orientation relationship with respect to miscut direction was observed in isostructural single crystal $SrRuO_3$ thin films on miscut (001) STO substrates.[9]

Single domain PSO templates were also fully strain relaxed after the three-step process. The in-plane and out-of-plane lattice parameters of the PSO films were determined from off-axis 400, 040, and 224 reflections. The lattice parameters of PSO on miscut (001) STO (α=1.0°) were a_o =5.60 Å, b_o=5.76 Å, and c_o=8.02 Å or a_o^p=4.02 Å and c_o^p =4.01 Å, which are very close to the reported bulk values,[1] within ±0.3% error, and therefore the PSO layer was considered fully relaxed. This degree of relaxation was the same for all PSO films regardless of substrate miscut angles or substrate materials (STO and LSAT).

Figure 3(a) shows high resolution x-ray diffraction θ–2θ scan of PSO-F films on miscut STO (α=1.0°). The only peaks detected are *d* spacing corresponding to (110) and (220), which was consistent with 2D area scans shown in Fig. 2(b). The out-of-plane crystalline quality of PSO was determined by the rocking curve scans of 220 reflections. The crystalline quality was significantly improved by the postannealing. The improvement of the rocking curve of PSO 220 reflection through the three-step process for PSO grown on α=1.0° STO is displayed in Fig. 3(b). The full widths at half maximum (FWHMs) of the rocking curves were 0.26°, 0.15°, and 0.066° for the PSO-B, PSO-AB, and PSO-F, respectively. The crystalline quality also significantly improved by the degree of miscut angle (α). In Fig. 3(c), the FWHM of the PSO 220 rocking curves versus miscut angle (α) is plotted parallel and perpendicular to the miscut direction. The optimal miscut angles were α=1.0° and 2.0° where the crystalline quality (FWHM ~0.06°) approached the STO substrate (FWHM ~0.02°).

Domain structure and crystal defects in the PSO film were studied by cross-sectional TEM. Figure 4(a) shows a bright field image of PSO on STO (α=1.0°), where the PSO-T and PSO-AB are identifiable by the observed planar boundary. The SAED pattern of the PSO-T layer is shown in Fig. 4(b), which corroborates the single in-plane and out-of-plane orientation of the PSO (110) domain. Figure 4(c) shows edge dislocation cores at the STO interface. Similar high temperature activation of dislocation diffusion towards the interface was observed in annealed BTO thin films on STO.[5,10] The primary mechanism for strain relaxation of the

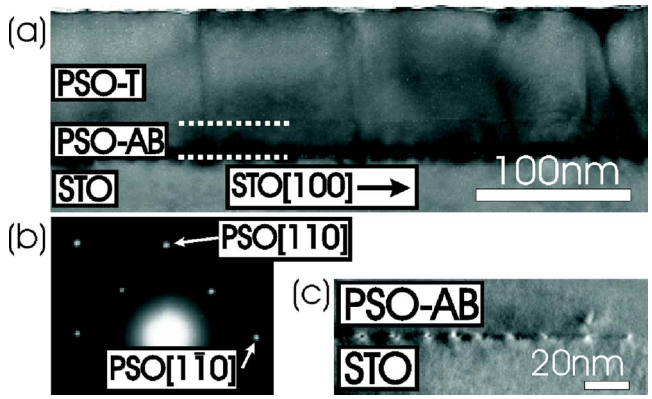

FIG. 4. (Color online) Bright field cross-sectional TEM image (a) of PSO on the miscut (001) STO substrate (α=1.0°) with the corresponding SAED (b) of the PSO-T layer and enlarged bright field image (c) of edge dislocation cores at the STO interface.

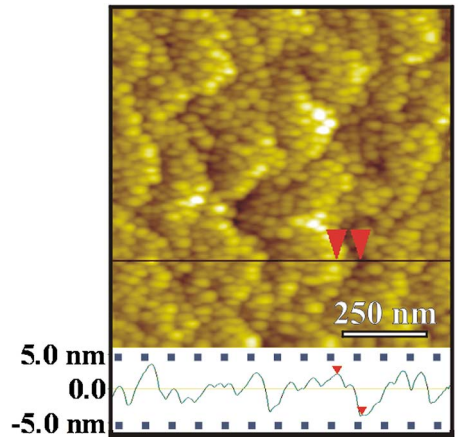

FIG. 5. (Color online) AFM image and section analysis of the PSO thin film on the miscut LSAT substrate with α=2.0°.

2.8% lattice mismatch between STO and PSO was the formation of edge dislocations. Burgers' vector of the misfit dislocations were determined to be $(100)a_{STO}$ by both electron diffraction contrast imaging and high resolution TEM (HRTEM). The statistical average spacing between dislocation cores was ~17 nm, which accounts for ~82% of the lattice mismatch where 14 nm spacing would be a perfect compensation.[11] Strain relaxation occurring at the STO interface eliminated dislocations near the surface region, which was corroborated with TEM in the PSO-T layer. Strain relaxed buffer layers with low defect density near the surface are ideal for heteroepitaxial growth of high quality multifunctional oxide thin films.

Vertical boundaries propagating through the PSO-AB and PSO-T layers were frequently observed [Fig. 4(a)]. SAED and HRTEM images determined that the boundaries were twist boundaries with small in-plane rotations. We believe that the twist boundaries originated from the growth and coalescence of smaller grains during annealing. The existences of these boundaries are consistent with the in-plane mosaic spread in high resolution XRD scans. The FWHM of off-axis azimuthal ϕ scans from the PSO 224 reflection were ~0.3° for PSO-F layers, independent of miscut angle. PSO-F on LSAT was ~0.5°, greater than PSO on STO. The in-plane mosaic spread, linked with the twist boundaries, may contribute to a partial strain relaxation.[12]

The surface morphology of the PSO-T layer was analyzed with an atomic force microscope (AFM) in contact mode. No particles were observed over a 10×10 μm^2 area scan. Figure 5 shows the surface morphology and section analysis of PSO on the LSAT (α=2.0°) substrate, which exhibits a three-dimensional island on terraces. The island growth is attributed to a strain relaxation due to a large lattice mismatch. Step bunching with step height of ~6 nm (~15 unit cells) can be seen. Miscut had the largest effect on the root mean square (rms) surface roughness due to step bunching. The PSO on the 1.0° miscut STO and the 4.0° miscut STO had a rms roughness of 1.2 and of 3.3 nm, respectively.

In summary, we have demonstrated that high quality single domain strain relaxed PSO can be deposited on STO and LSAT miscut substrates. The out-of-plane crystalline quality approaches the quality of bulk STO single crystals although the in-plane mosaic spread is significantly broader due to twist boundaries. Cross-sectional TEM and AFM shows dislocation-free and smooth surfaces. The strain relaxed templates of rare-earth scandates with controlled lattice parameters can be used for the fabrication of strain and domain engineered multifunctional oxide thin film devices.

This work was supported by ONR under Grant No. N000140510559 monitored by Colin Wood, the National Science Foundation under Grant Nos. DMR-0308012 and ECS-0210449, and a David & Lucile Packard Fellowship grant to one of the authors (C.B.E.). The authors thank Darrell Schlom for helpful discussions.

[1] J. Schubert, O. Trithaveesak, A. Petraru, C. L. Jia, R. Uecker, P. Reiche, and D. G. Schlom, Appl. Phys. Lett. **82**, 3460 (2003).
[2] K. J. Choi, M. Biegalski, Y. L. Li, A. Sharan, J. Schubert, R. Uecker, P. Reiche, Y. B. Chen, X. Q. Pan, V. Goplan, L.-Q. Chen, D. G. Schlom, and C. B. Eom, Science **306**, 1005 (2004).
[3] M. D. Biegalski, J. H. Haeni, S. Tolier-Mckinstry, D. G. Schlom, C. D. Brandle, and A. J. Ven Graitis, J. Mater. Res. **20**, 952 (2005).
[4] J. Wang and T. Y. Zhang, Appl. Phys. Lett. **86**, 192905 (2005).
[5] K. Terai, M. Lippmaa, P. Ahmet, T. Chikyow, H. Koinuma, M. Ohtani, and M. Kawasaki, Appl. Surf. Sci. **223**, 183 (2004).
[6] H. M. Christen, G. E. Jellison, Jr., I. Ohkubo, S. Huang, M. E. Reeves, E. Cicerrella, J. L. Freeouf, Y. Jia, and D. G. Schlom, Appl. Phys. Lett. **88**, 262906 (2006).
[7] G. Koster, B. L. Kropman, G. J. H. M. Rijnders, D. H. A. Blank, and H. Rogalla, Appl. Phys. Lett. **73**, 2920 (1998).
[8] E. Talik, M. Kruczek, H. Sakowska, and W. Szyrshi, J. Alloys Compd. **361**, 282 (2003).
[9] C. B. Eom, R. J. Cava, R. M. Fleming, Julia M. Phillips, R. B. van Dover, J. H. Marshall, J. W. P. Hsu, J. J. Krajewski, and W. F. Peck, Jr., Science **258**, 1766 (1992).
[10] H. P. Sun, X. Q. Pan, J. H. Haeni, and D. G. Schlom, Appl. Phys. Lett. **85**, 1967 (2004).
[11] H. P. Sun, W. Tian, X. Q. Pan, J. H. Haeni, and D. G. Schlom, Appl. Phys. Lett. **84**, 3298 (2004).
[12] J. W. Matthews, *Epitaxial Growth, Part B*, Edited by: J. W. Matthews, (Academic, New York, 1975), p. 556.